J|A|C|S
COMMUNICATIONS

Published on Web 10/30/2003

RNA Degradation in Cell Extracts: Real-Time Monitoring by Fluorescence Resonance Energy Transfer

Sarah A. Uhler, Dawen Cai, Yunfang Man, Carina Figge, and Nils G. Walter*
Department of Chemistry, University of Michigan, Ann Arbor, Michigan 48109-1055
Received June 23, 2003; E-mail: nwalter@umich.edu

The ability of an RNA molecule to persist in the cell among a plethora of ribonucleolytic activities is based on the tightly regulated relative rates of its synthesis and decay.[1] Regulation of specific mRNA turnover has long been studied, but the inability to derive rate constants with a convenient technique for directly monitoring RNA degradation has limited the introduction of predictive mathematical models.[2] In addition, the recent discovery of a multitude of short noncoding RNAs involved in gene regulation by RNA interference in eukaryotic genomes[3] and the advent of synthetic small interfering RNAs (siRNAs) for manipulating gene expression and probing gene function[4] have made an understanding of the rates and pathways of the cellular degradation of small RNA molecules indispensable.

Toward this goal, we have developed assays based on steady-state fluorescence resonance energy transfer (FRET) between two RNA-coupled fluorophores to observe nucleolytic decay of short synthetic RNAs (more precisely, RNA/DNA chimera) in real time, thus providing the desired kinetic rate information (Figure 1). Fluorescence-based assays have previously been used to measure the activity of purified RNases in vitro,[5] and fluorescent reporter proteins have been used to indirectly reflect cellular RNA abundance.[6] Our FRET assays are specifically designed to continuously monitor the partitioning between intact and degraded RNA in complex cellular mixtures. In addition, labeling with two fluorophores allows us to test the relative contributions of 5′ to 3′ and 3′ to 5′ exonucleolytic activities to RNA decay.

To study the effects of secondary structure on RNA decay we designed two 16-nucleotide (16 nt) oligonucleotides, RNAs **1** and **2**, that have similar base composition but have two very distinct secondary structures (Figure 1A). Additional design parameters included the incorporation of modified 2′-deoxy thymidines at nucleotide positions 3 and 13 for attachment of fluorescein and tetramethylrhodamine as a donor−acceptor FRET pair.[7] While RNA **1**, under our standard near-physiologic conditions (130 mM potassium glutamate, pH 7.5, 1 mM $MgCl_2$, 10 mM DTT, at 37 °C)[8] is predicted to reside >95% in the stem−loop secondary structure depicted in Figure 1A,[9] RNA **2** is expected to be completely unstructured (Figure 1a). These predictions were confirmed by UV and FRET melting experiments,[10] in which RNA **1** was found to melt at 64 and 61 °C without and with fluorophores attached, respectively, while RNA **2** showed no cooperative melting transition under these conditions.[11] Thus, the attachment of two fluorophores only slightly lowers the melting temperature of RNA **1**, indicating that it only insignificantly interferes with its secondary structure formation.

First, we determined the rate constants for in vitro degradation of RNAs **1** and **2** by RNase T_1 (Figure 1b), which cleaves 3′ to G.[12] RNA decay following addition of 0−250 nM RNase T_1 (pH 7.5) to 50 nM RNA **1** or **2** was monitored as a decrease in steady-state FRET signal (i.e., acceptor:donor fluorescence ratio) under standard conditions, and rate constants k_{dec} were extracted by single-exponential decay fits as described.[7,11] At all [RNase T_1] k_{dec} is greater for the unstructured RNA **2** than for the stem−loop of RNA **1** (Figure 1b). Furthermore, k_{dec} for RNA **1** approaches an asymptotic limit as [RNase T_1] reaches 4-fold excess over the RNA concentration, while k_{dec} for RNA **2** still increases. Fits of cooperative Hill binding equations to the data (Figure 1b) suggest stoichiometric (noncooperative) interaction of the enzyme with both RNAs, with rate constants at saturation of 3.9 min^{-1} for RNA **1** and ≥25 min^{-1} for the unstructured RNA **2** and apparent enzyme affinities K_M of 100 and 330 μM, respectively. Thus, the stem−loop structure of RNA **1** protects it from degradation by RNase T_1 relative to the unstructured RNA **2** (especially given that RNA **1** has more G's, potential RNase T_1 targets, inserted between the fluorophores).

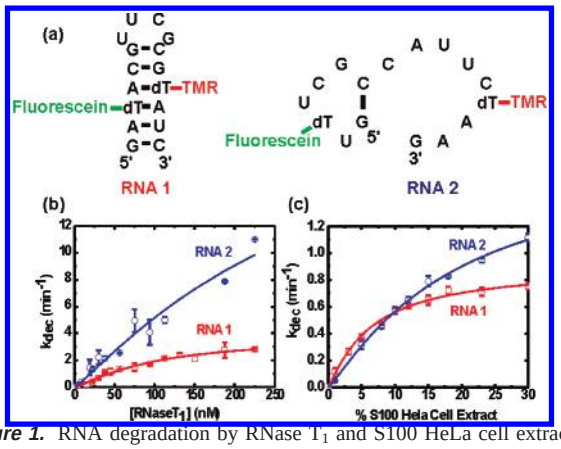

Figure 1. RNA degradation by RNase T_1 and S100 HeLa cell extract as monitored by FRET. (a) RNA folding software was used to predict the secondary structures of RNAs **1** and **2** of this study. The folding free energy of RNA **1** is favorable with −6.0 kcal/mol for a stem−loop structure, while RNA **2** folding is unfavorable at +2.6 kcal/mol.[9] (b,c) Decay rate constants k_{dec} were calculated for degradation of RNAs **1** and **2** by RNase T_1 and S100 HeLa cell extract. Solid lines, fits to the Hill equation.[11]

To show that this kinetic FRET assay also works in complex cellular mixtures, we studied the degradation of RNAs **1** and **2** in S100 cytosolic extract from HeLa cells, a common human epithelial cell line derived from cervix carcinoma. Again, we incubated the RNA under our standard near-physiologic conditions (130 mM potassium glutamate, pH 7.5, 1 mM $MgCl_2$, 10 mM DTT, at 37 °C),[8] then added increasing volume fractions of protease inhibitor treated cell extract (pH 7.6) and analyzed the resultant FRET decrease upon RNA decay as described above.[11] As with RNase T_1, the decay rate constant k_{dec} for RNA **1** approaches an asymptotic limit as the content of cell extract is raised to 30% (v/v), while that of RNA **2** does not (Figure 1c). Fits of the cooperative Hill binding equation to the data indicate noncooperative binding of one RNase enzyme in the cell extract to either RNA (Figure 1c). However, RNA **1** is degraded faster than RNA **2** at <10% (v/v) cell extract, yet slower at >10% (v/v). This results in rate constants at saturation of 0.90 min^{-1} and 1.76 min^{-1} for RNAs **1** and **2**, respectively, and apparent extract affinities of 6.4% (v/v) and 19% (v/v), respectively. Thus, the stem−loop structure of RNA **1** confers some RNase protection, but only at conditions close to the cellular

10.1021/ja036854b CCC: $25.00

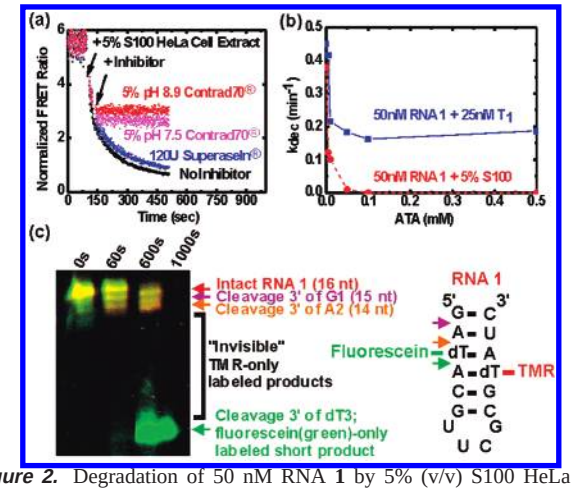

Figure 2. Degradation of 50 nM RNA **1** by 5% (v/v) S100 HeLa cell extract. (a) Contrad70 inhibits degradation by S100 HeLa cell extract, as evident from the lack of a FRET decrease after inhibitor addition, while SuperaseIn has minimal effects. (b) ATA is the most potent inhibitor of RNA **1** degradation by both RNase T_1 and S100 HeLa cell extract. (c) RNA **1** degradation by S100 HeLa cell extract, stopped at the indicated times and analyzed by gelFRET. Primary nuclease activity is that of a 5′ to 3′ exonuclease, as evident from the fluorescein−tetramethylrhodamine-labeled (yellow) 15 nt and 14 nt cleavage bands, followed by a size gap and release of a short fluorescein-only labeled (green) band, as indicated.

environment (highest % (v/v) cell extract). Competition experiments with unlabeled RNA show that the addition of RNA **2** interferes with the degradation of RNA **1** only when added to at least 100-fold excess (5 μM), indicating that the degradative pathways of structured and unstructured short RNAs are at least partially distinct. Similarly, poor competition is observed when adding excess RNA **1** to RNA **2**, suggesting that the observed saturation is due to an intrinsic limit of the decay rate constant, rather than titration of an essential degradative pathway component (data not shown).

To further characterize the utility of our FRET-based RNA decay assays, we tested their ability to report on known and potential RNase inhibitors. Divalent cations, such as Mg^{2+}, inhibit RNase T_1.[13] As expected, addition of increasing [Mg^{2+}] to 50 nM RNA **1** under otherwise standard conditions gradually decreases the rate constant of degradation by 75 nM RNase T_1 from 1.54 min^{-1} at 1 mM Mg^{2+} to 0.73 min^{-1} (that is, by 53%) at 500 mM Mg^{2+}, an effect that is prevented when Mg^{2+} is chelated by EDTA.[11] We also tested other potential inhibitors and found that addition of 10% Contrad70 (Decon Labs, Inc.), a strong, alkaline laboratory detergent, to a final pH of 9.3 inhibits RNase T_1 mediated RNA decay by 97%. Contrad70 at pH 7.5 inhibits by only 30%, consistent with the observation that a pH of 9.3 alone inhibits RNase T_1 already by 74%. Addition of 120 units of SuperaseIn (Ambion), a commercially available RNase T_1 inhibitor, was able to inhibit RNase T_1 by a mere 41%.[11]

To characterize the differences in nucleolytic activity of RNase T_1 and S100 cytosolic HeLa cell extract, the same inhibitors tested on RNase T_1 were added to RNA decay assays of 50 nM RNA **1** by 5% (v/v) cell extract (Figure 2a). Addition of 5% (v/v) Contrad70 inhibits degradation at a final pH of 7.5 and 8.9 by 75 and 97%, respectively (Figure 2a). SuperaseIn (120 units) inhibits cell extract-mediated RNA decay by only 17% (Figure 2a), a substantially smaller extent of inhibition than that observed for RNase T_1. Likewise, up to 500 mM Mg^{2+} does not appreciably inhibit degradation of RNA **1** by cell extract (data not shown), indicating that the major nuclease activity found in S100 cytosolic HeLa cell extract is distinct from RNase T_1 activity. However, in aurin tricarboxylic acid (ATA), a neuroprotective compound and known RNase inhibitor,[14] we found a strong inhibitor of both RNase T_1 and S100 cytosolic HeLa cell extract at pH 7.4 (Figure 2b). We also found it to slightly alter the fluorescence emission profiles of our doubly labeled RNAs, consistent with lower-energy transfer between the donor and acceptor dyes.[11] This suggests that ATA may bind to RNA and alter its secondary structure, thus protecting it from degradation by RNases.

Finally, we utilized inhibition by 10% Contrad70 at pH 9.3 to stop RNase degradation. Reaction products were then analyzed at defined times by 20% denaturing, 7 M urea, polyacrylamide gel electrophoresis, and gelFRET analysis.[15] All possible RNase T_1 cleavage sites were observed for RNA **1**, although cleavage 3′ to G1 and G12 occurred preferentially over cleavage 3′ to G6 and G10 (data not shown). Cleavage at both potential sites was observed for RNA **2**, although cleavage after G1 occurred more rapidly than cleavage after G6 (data not shown), demonstrating a general preference for terminal over internal cleavage sites. Similar experiments using S100 cytosolic HeLa cell extract showed that 5′ to 3′ exonuclease is the predominant RNase activity in the extract for both RNA **1** (Figure 2c) and RNA **2** (data not shown), as is typical for decapped RNA.[1] Degradation was completed by 1000 s, which coincides with our FRET kinetics (Figure 2c).

Here, we have demonstrated the utility of a novel FRET assay to monitor in real-time the degradation kinetics of short RNAs by a purified RNase and in S100 cytosolic HeLa cell extract. We find that single-stranded RNA **2** is degraded more rapidly than the stem−loop RNA **1** under all conditions tested except for low concentrations of cell extract. Furthermore, our assay allows for the observation of in-assay inhibition of the RNase activity using inhibitors such as Contrad70 and ATA. Observation of the exact sites of cleavage using gelFRET confirmed that the change in FRET was a result of nucleolytic activity. Extension of these methods to living cells to probe cellular processes involving short RNAs, such as siRNAs, is under active investigation.

Acknowledgment. This work was supported by NIH Grant GM62357, ACS-PRF Grant 37728-G7, and a Dow Corning endowment. We thank Tom Kerppola for use of his FluorImager, and David Engelke and Danny Reinberg for HeLa cell extract.

Supporting Information Available: Details of RNA synthesis, fluorescence methods, and additional figures (PDF). This material is available free of charge via the Internet at http://pubs.acs.org.

References

(1) (a) Deutscher, M. P.; Li, Z. *Prog. Nucleic Acid Res. Mol. Biol.* **2001**, *66*, 67−105. (b) Hollams, E. M.; Giles, K. M.; Thomson, A. M.; Leedman, P. J. *Neurochem. Res.* **2002**, *27*, 957−980. (c) Tourriere, H.; Chebli, K.; Tazi, J. *Biochimie* **2002**, *84*, 821−837.
(2) Cao, D.; Parker, R. *RNA* **2001**, *7*, 1192−1212.
(3) Hannon, G. J. *Nature* **2002**, *418*, 244−251.
(4) McManus, M. T.; Sharp, P. A. *Nat. Rev. Genet.* **2002**, *3*, 737−747.
(5) Trubetskoy, V. S.; Hagstrom, J. E.; Budker, V. G. *Anal. Biochem.* **2002**, *300*, 22−26.
(6) Chen, C. A.; Cowan, J. A. *Chem. Commun.* **2002**, *3*, 196−197.
(7) (a) Walter, N. G. *Methods* **2001**, *25*, 19−30. (b) Walter, N. G.; Harris, D. A.; Pereira, M. J.; Rueda, D. *Biopolymers* **2002**, *61*, 224−242. (c) Walter, N. G. *Curr. Protocols Nucleic Acid Chem.* **2002**, *11.10*, 11.10.11−11.10.23. (d) Pereira, M. J.; Harris, D. A.; Rueda, D.; Walter, N. G. *Biochemistry* **2002**, *41*, 730−740. (e) Harris, D. A.; Rueda, D.; Walter, N. G. *Biochemistry* **2002**, *41*, 12051−12061. (f) Jeong, S.; Sefcikova, J.; Tinsley, R. A.; Rueda, D.; Walter, N. G. *Biochemistry* **2003**, *42*, 7727−7740.
(8) Christensen, K. A.; Myers, J. T.; Swanson, J. A. *J. Cell Sci.* **2002**, *115*, 599−607.
(9) (a) Mathews, D. H.; Sabina, J.; Zuker, M.; Turner, D. H. *J. Mol. Biol.* **1999**, *288*, 911−940. (b) Zuker, M. *Curr. Opin. Struct. Biol.* **2000**, *10*, 303−310. (c) SantaLucia, J. *Proc. Natl. Acad. Sci. U.S.A.* **1998**, *95*, 1460−1465.
(10) Vamosi, G.; Clegg, R. M. *Biochemistry* **1998**, *37*, 14300−14316.
(11) See Supporting Information.
(12) Deshpande, R. A.; Shankar, V. *Crit. Rev. Microbiol.* **2002**, *28*, 79−122.
(13) Takahashi, K.; Uchida, T.; Egami, F. *Adv. Biophys.* **1970**, *1*, 53−98.
(14) Baba, M.; Schols, D.; Pauwels, R.; Balzarini, J.; De Clercq, E. *Biochem. Biophys. Res. Commun.* **1988**, *155*, 1404−1411.
(15) Ramirez-Carrozzi, V. R.; Kerppola, V. K. *Methods* **2001**, *25*, 31−43.
JA036854B